

Enhanced Crystallographic incorporation of Strontium(II) ions to Calcite via Preferential Adsorption at Obtuse Sites during Spiral Growth

Supporting Information

David J. Hodkin[†], Douglas I. Stewart[‡], James T. Graham[§], Giannantonio Cibin[◇], Ian T. Burke^{†*}

[†]School of Earth and Environment, University of Leeds, Leeds, LS2 9JT, UK.

*Corresponding Author's E-mail: i.t.burke@see.leeds.ac.uk; Phone: +44 113 3437532; Fax: +44 113 3435259

[‡]School of Civil Engineering, University of Leeds, Leeds, LS2 9JT, UK

[§]National Nuclear Laboratory, Sellafield, Cumbria, CA20 1PG, UK

[◇]Diamond Light Source, Harwell Science and Innovation Campus, Didcot, OX11 0DE, UK

S.I. Section 1 - XRD Carbonate Polymorphism

Initial constant composition experiments were carried out in a continuous tank stirred reactor fed by a $\text{Ca}(\text{OH})_2/\text{SrCl}_2$ solution (in which the Sr:Ca ratio varied from 0-0.48) and a 50 mM Na_2CO_3 solution. This achieved a constant composition environment in which the Sr/Ca ratio varied, enabling observations to be made on the role of solution Sr/Ca on Sr incorporation into calcite. Reactions were carried out in a 150 mL reaction vessel in the absence of initial seed crystals.

Data compiled in SI Table 1 show a significant variation in the polymorphism of the carbonate forming. At high Sr:Ca (0.48) strontianite becomes the main phase however below this value a mixture of calcite and aragonite was present, the proportions of which show no systematic variation.

A potential explanation for this is that both calcite and aragonite have similar solubility products (3.39×10^{-9}) and (4.57×10^{-9}) respectively. Due to these similar supersaturations, and the lack of seed crystals, the polymorph distribution will be dependent of the first phases nucleated in solution. If a significant proportion of the early-formed crystals are of the aragonite polymorph then this will act as a seed crystal allowing a significant proportion of aragonite to form. Due to calcites slightly higher supersaturation this is the most common phase to nucleate which is represented by the skew of the data towards calcite.

SI Table 1. XRD data from the unseeded CTSR experiments

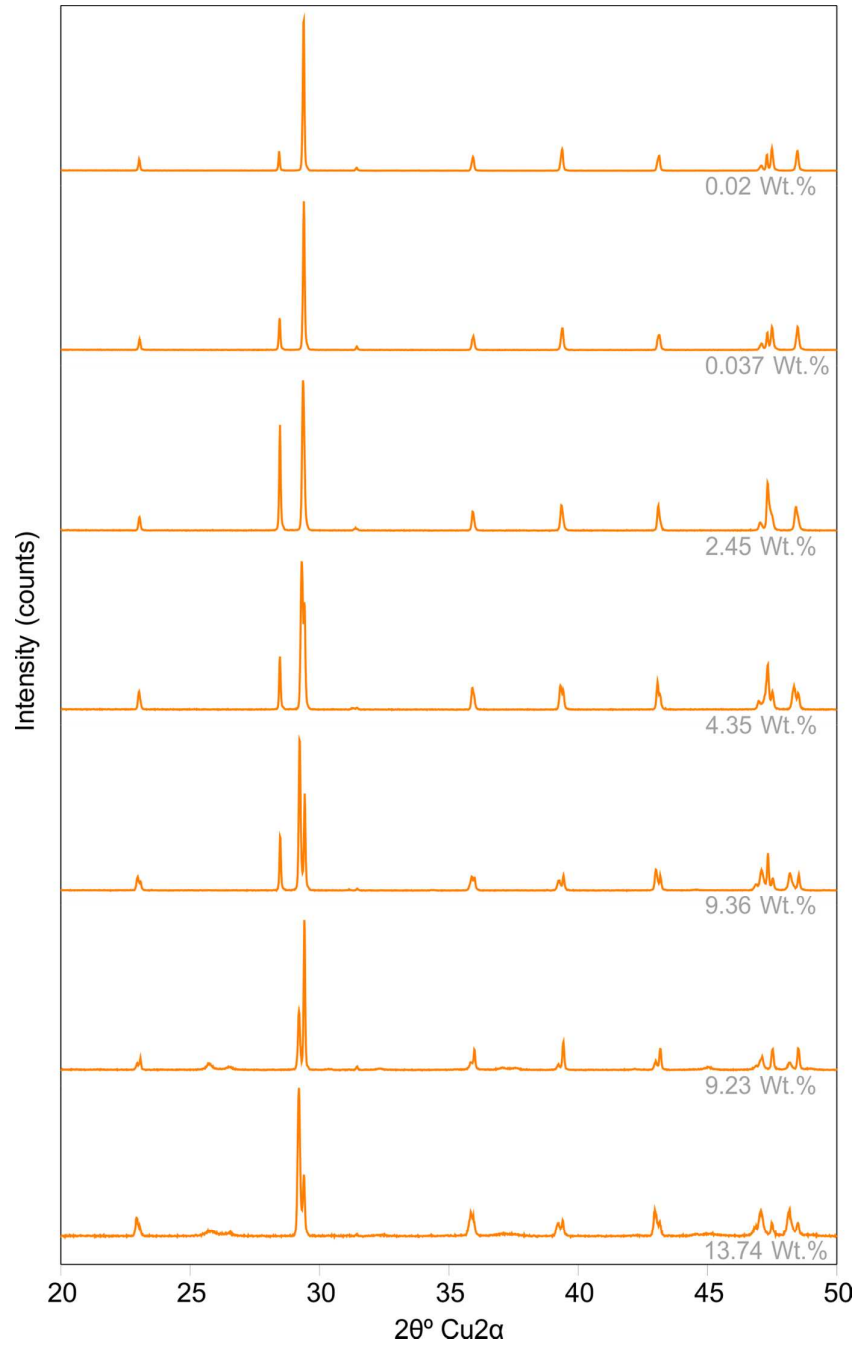
Sample #	[Ca] (mM)	[Sr] (mM)	Sr/Ca X10 ²	Calcite %	Aragonite %	Strontianite %
2	15	0	0	98.67	1.33	0
8	10	0	0	81.29	18.71	0
9	10	0	0	12.40	87.6	0
13	14.9	0.1	0.01	73.39	26.61	0
3	9.9	0.1	0.01	93.39	6.37	0.24
14	14.5	0.5	0.03	98.53	1.44	0.03
4	9.5	0.5	0.05	100	0	0
17	12	3	0.25	97.23	1.98	0.79
6	8	2	0.25	98.85	0.51	0.64
7	6.3	3	0.48	24.87	26.1	49.03
12	9.5	0.5	0.05	-	-	-
15	14	1	0.07	-	-	-
5	9	1	0.11	-	-	-
16	13	2	0.15	-	-	-
18	7.5	2.5	0.33	-	-	-

Experiments were repeated with rhombohedral calcite seed crystals to guide the crystallization pathways. This was successful at producing a 100% Calcite precipitate in most experiments however XRD data was collected on a Bruker D8 XRD with a Cu K α source for selected experiments from the series, it was not possible to collect XRD data for all experiment due to sample size constraints. A summary of samples with XRD data collected is included in the table below, with XRD traces in SI Fig. 3. Two samples were identified with XRD peaks at 25.7 and 26.5 which are consistent with strontianite although a shift to higher 2 θ values was observed, potentially indicating Calcite substitution into the lattice.

SI Table 2. Identification of carbonate polymorph via XRD for selected samples from the unseeded constant composition experiments. C=Calcite, S=Strontianite.

#	Sr/Ca sol	Sr/Ca ppt	Wt.% Sr	Dsr	XRD	SI_Cal	SI_Str
50	0	0	0.02	0.1	C	1.26	-0.53
65	0.01	0	0.11	0.11		1.07	0.09
66	0.02	0	0.21	0.13		1.36	0.59
58	0.03	0	0.32	0.11		1.3	0.76
57	0.04	0	0.37	0.12	C	1.24	0.75
51	0.04	0.01	0.5	0.13		1.24	0.85
59	0.2	0.02	1.96	0.12		1.28	1.54
52	0.22	0.03	2.45	0.13	C	1.12	1.43
60	0.39	0.04	3.59	0.11		1.21	1.76
53	0.42	0.05	4.35	0.13	C	1.26	1.85
55	0.46	0.13	9.23	0.28	C/S	2.07	2.69
61	0.57	0.08	6.36	0.14		1.21	1.93

67	0.74	0.11	8.3	0.15		1.1	1.94
63	0.74	0.13	9.48	0.17		1.33	2.16
56	0.84	0.2	13.74	0.24	C/S	1.34	2.22
62	0.85	0.32	19.04	0.38		1.4	2.29
54	0.86	0.13	9.36	0.15	C	1.14	2.04



SI Figure 1. XRD data for 7 samples from the unseeded constant composition experiments

S.I. Section 2 - Specific Surface Area of Calcite Seed Crystal

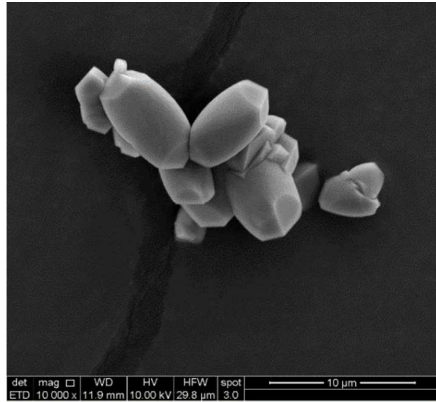
The surface area of calcite seed crystals was determined by triplicate BET analysis using a Micromeritics Gemini VII 2390a instrument. A sample of calcite powder was weighed and dried overnight at a temperature of 105°C under a nitrogen atmosphere to remove any water, after which the sample was reweighed. A dead-space volume measurement was taken using helium which was then removed via vacuum and triplicate measurements were taken, using nitrogen as an absorbent at -196 °C. An average value of 0.206 m² L⁻¹ was observed. By adding a mass of 0.73 g of the seed to the 150 mL reactor a surface area of 1 m² L⁻¹ was achieved.

Table 1 BET surface area data

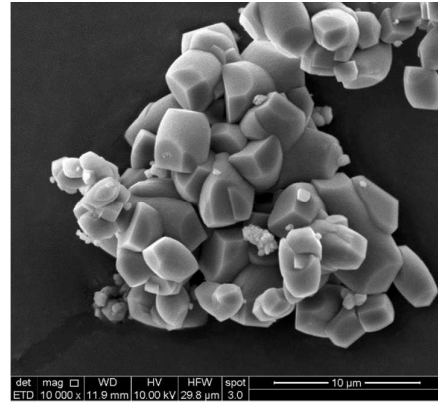
	BET surface area (m ² g ⁻¹)	BET Constant (C)	r ²
a	0.208	-122	0.999
b	0.206	-108	0.999
c	0.206	-106	0.999
Average	0.206	-112	0.999

S.I. Section 3 - Calcite morphology series

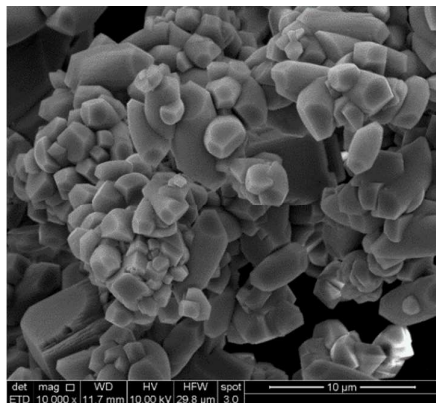
The following 5 images were collected on a FEI Quanta 650 Field Emission Gun SEM, from a suite samples with Wt. % Sr ranging from 0.02-9.36%. These images focus on the elongate morphology, displaying its elongating with greater Sr incorporation.



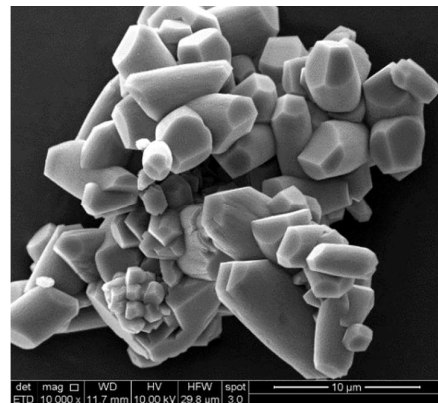
0.02 Wt. % Sr



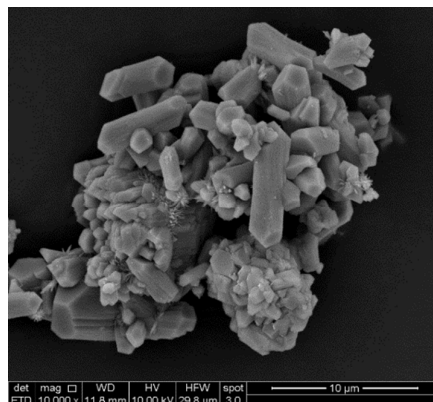
0.37 Wt. % Sr



2.45 Wt. % Sr



4.35 Wt. % Sr

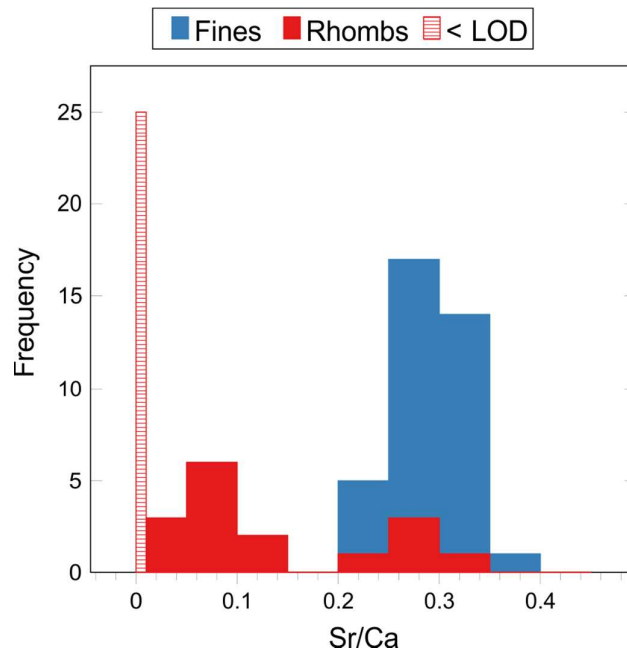


9.36 Wt. % Sr

SI Figure 2. Increase of the W/L of the elongate crystals with increasing Wt. % Sr

S.I. Section 4 - EDS Histogram

EDS spot analyses were carried out over 41 Rhombic crystals and 37 Crystals of fine material which presented as either elongate crystals or circular in cross section. Of the 41 Rhombic crystals 25 displayed no strontium above limits of detection while the remaining 16 displayed a median Sr/Ca of 0.019. All of the fine material registered Sr at concentrations above the LOD, with a median Sr/Ca of 0.25. This is displayed in the histogram in SI Figure 3.



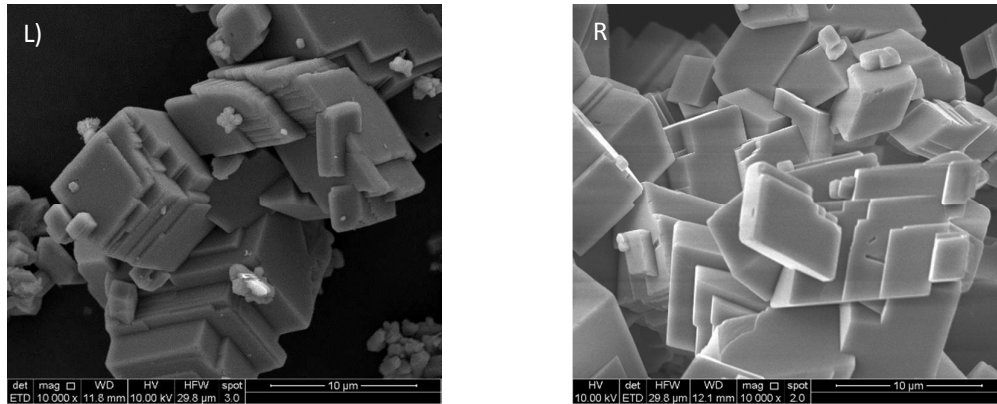
SI Figure 3. Sr/Ca ratios from EDS spot analysis of a resin embedded sample of precipitate containing 6.36 Wt. % Sr

SI Table 2, Width to Length ratios for selected samples from the seeded CTSR experimental series.

	Wt. % Sr	L (μm)	W (μm)	L/W
Elongate	0.02	4.00	2.50	1.59
	0.37	3.73	2.39	1.61
	2.45	3.00	1.65	1.82
	4.35	4.00	1.89	2.13
	9.36	3.48	1.38	2.50
	\bar{x}	3.64	1.96	1.86
Rhombic	\bar{x}	6.86	5.97	1.15

S.I. Section 5 - Rhombic Crystal Comparison

These micrographs are included to demonstrate the similarity in morphology of the seed crystals used at the start of the reaction and the rhombic morphology obtained at the completion of the reaction.



SI Figure 4 Comparison of Rhombic crystal obtained from the seeded CTSR (L) and a sample of the seed crystals added at $t=0$ (R)

S.I. Section 6 – Data table

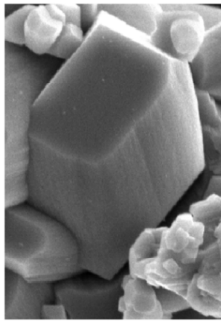
The final two experiments (56 and 62) were excluded from analyses as these displayed distribution coefficients indicative of strontianite formation. XRD analysis was carried out on sample 56 which returned a positive analysis for strontianite.

Table 3 Activities, saturation indices and ionic strength were calculated using PHREEQC and assuming Na and Cl are behaving conservatively. $SI_{\text{Calcite}} = 10^{8.48}$ $SI_{\text{Strontianite(Pmcn)}} = 10^{-9.26}$ $SI_{\text{Strontianite(R3C)}} = 10^{-7.6}$ taken from (Kulik et al., 2010).

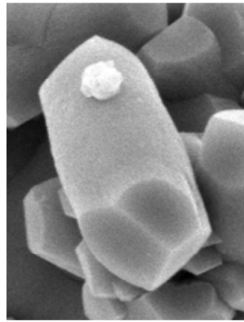
#	Ca (mM)	Sr (mM)	TIC (mM)	a(Ca ⁺²) (mM)	a(Sr ⁺²) (mM)	a(CO ₃ ⁻²) (mM)	Sr/Ca (Solution)	Ca/CO ₃ (Solution)	Sr/Ca (ppt)	Wt. % (ppt)	DSr	SI _{Calcite} (R3c)	SI _{Strontianite} (Pmcn)	SI _{Strontianite} (R3c)	Ionic Strength mmol/L	pH	Temp (°C)	Rate mmol/h
50	1.74	0.00	0.05	0.88	0.00	0.02	0.00	33.68	0.00	0.02	0.13	1.43	-0.54	-2.20	15.11	12.17	20.97	0.834
65	1.81	0.02	0.03	0.91	0.01	0.01	0.02	56.73	0.00	0.11	0.11	1.24	0.08	-1.58	15.36	12.22	21.30	0.781
66	1.82	0.03	0.06	0.91	0.02	0.02	0.04	29.76	0.01	0.21	0.13	1.53	0.58	-1.08	15.41	12.19	21.07	0.788
58	2.26	0.07	0.04	1.11	0.04	0.01	0.07	52.59	0.01	0.32	0.11	1.47	0.75	-0.91	16.67	12.24	21.07	0.837
57	2.04	0.07	0.04	1.02	0.04	0.01	0.08	48.73	0.01	0.37	0.12	1.41	0.74	-0.92	16.10	12.24	21.00	0.904
51	1.51	0.07	0.06	0.77	0.04	0.02	0.10	26.68	0.01	0.50	0.13	1.41	0.84	-0.82	14.72	12.06	12.06	1.099
59	1.74	0.35	0.05	0.88	0.20	0.02	0.44	32.69	0.05	1.96	0.12	1.45	1.53	-0.13	16.16	12.22	20.70	0.916
52	1.39	0.31	0.05	0.71	0.18	0.02	0.49	30.15	0.06	2.45	0.13	1.29	1.42	-0.24	15.12	12.03	21.10	0.959
60	1.74	0.68	0.05	0.87	0.38	0.02	0.85	37.71	0.10	3.59	0.11	1.38	1.75	0.09	17.13	12.20	21.03	0.882
53	1.38	0.58	0.06	0.70	0.33	0.02	0.93	21.26	0.12	4.35	0.13	1.43	1.84	0.18	15.89	12.02	21.27	0.979
61	1.77	1.01	0.05	0.88	0.56	0.02	1.24	39.18	0.18	6.36	0.14	1.38	1.92	0.26	18.19	12.18	20.73	0.862
67	1.45	1.08	0.04	0.73	0.61	0.01	1.63	33.82	0.24	8.30	0.15	1.28	1.93	0.27	17.56	12.11	21.03	0.755
54	1.17	1.01	0.06	0.61	0.58	0.02	1.89	20.18	0.28	9.36	0.15	1.32	2.03	0.37	16.63	12.09	17.83	0.807
63	1.73	1.28	0.06	0.86	0.71	0.02	1.62	28.75	0.28	9.48	0.17	1.50	2.15	0.49	18.89	12.12	21.00	0.742
56	1.71	1.43	0.06	0.86	0.79	0.02	1.84	27.20	0.45	13.74	0.24	1.51	2.21	0.55	19.32	12.13	21.17	0.848
62	2.25	1.91	0.05	1.09	1.02	0.01	1.86	41.38	0.70	19.04	0.38	1.57	2.28	0.62	22.15	12.09	20.93	0.667

S.I. Section 7 – Crystallography

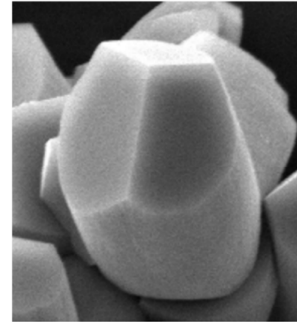
Line drawings of selected crystals were extracted from selected SEM micrographs. The interfacial angles between these faces appears to be $>90^\circ$ although it is difficult to precisely measure the angles as the none of the facets are viewed face on by the SEM. The apex of each crystal clearly showed three main faces with one larger than the other two, it was assumed that this was the $\{104\}$ face.



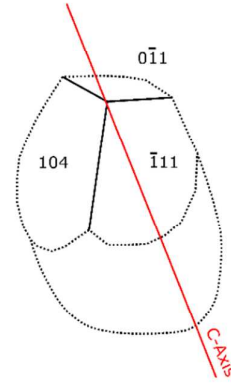
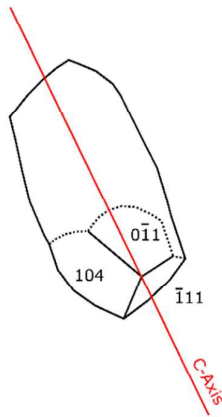
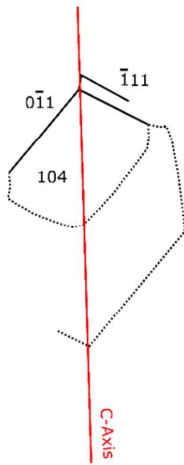
5 μm



5 μm



5 μm



Interfacial Angles all >90

SI Figure 5 Crystal line drawings displaying C-Axes and crystal faces.